APPARATUS ARCHITECTURE OF THE CONODONT *NICORAELLA KOCKELI* (GONDOLELLOIDEA, PRIONIODININA) CONSTRAINS FUNCTIONAL INTERPRETATIONS

by JINYUAN HUANG[1,2,3,4*], CARLOS MARTÍNEZ-PÉREZ[2,5*], SHIXUE HU[1], QIYUE ZHANG[1], KEXIN ZHANG[3], CHANGYONG ZHOU[1], WEN WEN[1], TAO XIE[1], MICHAEL J. BENTON[5], ZHONG-QIANG CHEN[6], MAO LUO[7], *and* PHILIP C. J. DONOGHUE[5*]

[1]Chengdu Center of China Geological Survey, Chengdu 610081, China; hjinyuan@cgs.cn

[2]Cavanilles Institute of Biodiversity and Evolutionary Biology, University of Valencia, 46980, Valencia, Spain; Carlos.Martinez-Perez@uv.es

[3]Institute of Geological Survey, China University of Geosciences (Wuhan), Wuhan 430074, China

[4]State Key Laboratory of Palaeobiology and Stratigraphy (Nanjing Institute of Geology and Palaeontology, CAS), Nanjing, 210008, China

[5]School of Earth Sciences, University of Bristol, Life Sciences Building, Tyndall Avenue, Bristol, BS8 1TH, UK; phil.donoghue@bristol.ac.uk

[6]State Key Laboratory of Biogeology and Environmental Geology, China University of Geosciences, Wuhan 430074, China

[7]State Key Laboratory of Palaeobiology and Stratigraphy, Nanjing Institute of Geology and Palaeontology and Center for Excellence in Life and Paleoenvironment, Chinese Academy of Sciences, 39 East Beijing Road, Nanjing 210008, China

[*]Corresponding authors

Abstract: We reconstruct the apparatus architecture of the gondollelid conodont *Nicoraella kockeli* based on fused clusters from the early Middle Triassic (middle Anisian, Pelsonian) of Luoping County, east Yunnan Province, southwest China. These materials were characterized non-invasively using Synchrotron X-Ray Tomographic Microscopy and the ensuing data analysed using computed tomography, allowing us to infer the composition, homologies and architectural arrangement of elements within the apparatus. Much of the original three-dimensional architecture of the apparatus is preserved and our apparatus reconstruction is the best characterized of any taxon within the superfamily Gondolelloidea. This allows us to test architectural models for gondolelloids and prioniodinins, more generally, as well as the functional interpretations based upon them. In particular, we reject a recent functional interpretation of the conodont feeding apparatus which was based on a biomechanically-optimised inference of apparatus architecture in a close gondolelloid relative of *Nicoraella*. Nevertheless, our architectural model provides a foundation for future functional interpretations of gondolleloids and prioniodinins, more generally.

Key words: structure, function, conodont apparatus, Middle Triassic, SW China

CONODONTS are among the most diverse clades of jawless vertebrates and they are abundant components of Palaeozoic and early Mesozoic marine ecosystems. However, their role within those ecosystems has been unclear because of controversy surrounding the functional interpretation of their feeding apparatus which comprised the eponymous tooth-like elements that dominate the conodont fossil record. Conodont functional morphology has a long history of poorly constrained speculation and, indeed, for much of this time, debates over the affinity of conodonts and the function of their elements were inextricably linked. The identification of conodont element-like structures in diverse metazoans, plants and even fungi inspired both functional interpretations of the elements and phylogenetic interpretations of the host organism (Aldridge 1987). Separation of debates over affinity and function awaited the discovery of soft tissue remains of conodonts (Briggs and Fortey 1982), but subsequent research demonstrated that it had always been possible to independently constrain, develop, and test hypotheses of element function based on articulated skeletal assemblages that preserve the collapsed remains of the feeding apparatus of a single conodont individual (Aldridge *et al.* 1987, 1995, 2013; Purnell and Donoghue 1997, 1998, 1999).

First discovered in the early 1930s (Schmidt 1934; Scott 1934), 'natural assemblages' preserve elements of different morphology in a limited series of different relative arrangements, interpreted originally to reflect postmortem muscle and ligament contortion and contraction (Collinson *et al.* 1972). These arrangements were subsequently shown to reflect different collapse orientations of the same original three-dimensional construction, that can be 'solved' by a three dimensional physical model which, when viewed from different perspectives, simulates the relative arrangement of elements in natural assemblages and, thus, the original orientation of collapse (Aldridge*, et al.* 1987). Such models have been built for disparate conodont clades, demonstrating collectively that the natural assemblages of most 'complex conodonts' can be explained by the model derived from *Idiognathodus* (Purnell and Donoghue 1997). More recently, a different architectural arrangement was inferred for the Early Triassic *Novispathodus*, interpreted to reflect different element positions within a functional cycle (Goudemand *et al.* 2011). This architecture was based in part on a heuristic biomechanical analysis of the optimal functional and positional arrangement of elements, inspired by partial fused natural assemblages of *Novispathodus* and complete but compressed bedding plane natural assemblages of *Neogondolella* (Goudemand *et al.* 2011). Overall, their analysis suggests that different conodont taxa exhibit different element architectures.

Here, we reconstruct the apparatus of *Nicoraella kockeli* based on a collection of fused natural assemblages from the early Middle Triassic (middle Anisian, Pelsonian) of Luoping County, east Yunnan Province of southwest China (Huang *et al*. 2018a, b). *Nicoraella kockeli* is a close relative of *Novispathodus* and *Neogondolella*, allowing us to test the architectural and functional models proposed by Goudemand *et al.* (2011). We find that the functional model presented by those authors contradicts primary anatomical evidence in the fossils from which it was derived. As such, both should be rejected. Finally, we present an accurate reconstruction of the feeding apparatus of *Nicoraella* and consider implications of its apparatus architecture for hypotheses of function.

MATERIALS AND METHODS

Our study is based on four articulated clusters from the Luoping Konservat-Lagerstätte in Luoping County, Yunnan Province, southwestern China. The Luoping Biota encompasses a diverse assemblage of microfossils (conodonts, foraminifers, ostracods, etc.) as well as articulated macrofossils including nektonic marine reptiles and fishes, and benthic echinoderms (crinoids, sea urchins, sea cucumbers, and sea stars), bivalves, gastropods, belemnoids, ammonoids, brachiopods, arthropods (decapods, isopods, limulus, and cycloids), as well as trace fossils and a few terrestrial plants and millipedes (Hu *et al.* 2011).

The fossiliferous sediments occur in the Guanling Formation (Member II), which is composed, in succession, of a dark micritic nodular limestone, followed by a micrite bearing chert nodules or siliceous bands, followed by a micrite with dolomite (Zhang *et al.* 2009). The clusters come from several limestone layers in the lower thin-bedded unit of the Dawazi Section, which consists mainly of thin laminar micritic limestone intercalated with prominent cherty nodules. It is dated to the Pelsonian Substage of the Anisian (Middle Triassic), based upon the presence of the conodont *Nicoraella kockeli* (Huang *et al.* 2009, 2011).

The element clusters attributable to *Nicoraella kockeli* were obtained through acid digestion (6% acetic acid) of the limestone samples. The clusters are preserved in only a partially compressed state (Figs 1–5), maintaining considerable three dimensionality in the arrangement of the elements which are bound together by diagenetic calcium phosphate (Figs 2–5). All specimens are deposited at the Chengdu Center of China Geological Survey (CDCGS). The most complete clusters were characterized using synchrotron-radiation X-Ray Tomography (SRXTM) on the X02DA TOMCAT beamline at the Swiss Light Source, Paul Scherrer Institute (Villigen, Switzerland), a nondestructive technique that

permitted us to establish the morphology and relative arrangement of the elements comprising the clusters using computed tomography (Donoghue *et al.* 2006). The samples were scanned using a 20x objective, at 10-17 KeV with an exposure time of 180–350 ms, acquiring 1501 projections equiangularly over 180°. Projections were post-processed and rearranged into flat- and dark-field-corrected sinograms, and reconstruction was performed on a 60-core Linux PC farm using a Fourier transform routine and a regridding procedure (Marone *et al.* 2010). The resulting volume has isotropic voxel dimensions of 0.325 µm. Slice data were analysed and manipulated using the computed tomography software Avizo 8 (fei.com). Finally, renderings were manipulated using the software Geomagic Studio ver. 12 (Geomagic, Rock Hill, SC, USA) to reconstruct digitally the apparatus structure and simulate the different collapse orientations represented by the fused natural assemblages.

Previously, researchers have inferred apparatus architecture through physical modeling, arriving at a single solution that, when viewed from different orientations, simulates the collapse orientation represented in the natural assemblages (Aldridge*, et al.* 1987, 1995, 2013; Purnell and Donoghue 1997, 1998). We followed an analogous approach, building a digital three-dimensional model based on the virtual elements segmented using computed tomography from the tomographic characterizations of the cluster preserving the largest number of elements [pm028-18-wy1-C1; Fig. 2A–C]. Following the physical modelling approach, we adjusted the relative arrangement of the elements until we arrived at a single model in which the core aspects of element arrangement could be replicated by viewing the virtual model from different orientation, simulating the direction of collapse. Though we had access to many tens of fused natural assemblages (Huang*, et al.* 2018a), only a small number of these were composed of enough of the apparatus to prove useful in reconstructing the original apparatus architecture. Furthermore, these assemblages preserve a limited number of collapse orientations and, therefore, perspectives on the apparatus – by their nature, complete fused clusters are limited to orientations in which all of the elements overlap another, or else they will not be fused together (Huang*, et al.* 2018a). However, a number of the clusters exhibit limited collapse, preserving aspects of the original spacing and relative arrangement of the elements within the apparatus, not usually seen in fused cluster natural assemblages (Nicoll 1982, 1985; Nicoll and Rexroad 1987; Mastandrea *et al.* 1997; Schülke 1997; Goudemand*, et al.* 2011). Nevertheless, we reconstructed the apparatus by first arranging the elements of *Nicoraella kockeli* according to the architecture of *Polygnathoides* (Purnell and Donoghue 1998) before adjusting the relative position and orientation of the elements to simulate the collapse orientations of the fused cluster natural assemblages of *N. kockeli.*

Following Purnell *et al.* (2000), we describe the orientation of elements and element processes with reference to their traditional within-element orientations ('anterior', 'posterior', etc., with reference to the cusp) and their natural biological orientations (rostral-caudal, dorsal-ventral, sinistral-dextral), with reference to the orientation of homologous elements in specimens of *Clydagnathus winsorensis* preserving soft tissue anatomy, from the Mississippian Granton Shrimp Bed of Granton, Edinburgh (Aldridge *et al.* 1993).

RESULTS

Cluster composition

Four clusters were characterised using SXRTM. These differ in terms of the number of elements present, with one cluster composed of 15 elements (Fig. 2), another of 13 (Fig. 3), and two clusters composed of 11 elements each (Figs 4, 5). All four clusters are composed of 11 ramiform elements, including five symmetrical pairs of elements and a single, central, approximately symmetrical alate element. Two of the clusters possess an additional symmetrical pair of elements of pectiniform morphology, while the cluster composed of 15 elements has a second pair of pectiniform elements. The relative arrangement of the component elements differs between clusters, comparable to those described previously from natural assemblages (Purnell and Donoghue 1998), and we interpret them as reflecting different collapse orientations of the same original three-dimensional arrangement of elements (Briggs and Williams 1981; Aldridge*, et al.* 1987). A detailed description of the fused cluster natural assemblages is provided by Huang *et al.* (2018a, b).

Apparatus composition

The inferred architectural model allows us to identify the homology of the component elements directly, based on their positions within the apparatus (Fig. 1; Purnell*, et al.* 2000), rather than on the basis of similarity in element morphology to taxa in which position homologies can be observed. Huang *et al*. (2018a, b) established that the apparatus of *Nicoraella* is composed of 15 elements (Fig. 1), including a pair of caudal pectiniform P_1 elements and a more rostral pair of pectiniform P_2 elements that overlap on the rostro-caudal axis with an array of ramiform elements. The ramiform array is composed of an alate axial S_0 with a short lateral process and a long posterior process extending from the cusp. Abaxially, in order relative to the S_0, are symmetrical sinistral and dextral pairs of (i) breviform dygyrate S_1 elements with a short antero-lateral process aligned ventrally, a caudally-directed cusp, and a long inner-lateral process that extends rostrally; (ii) breviform digyrate S_2 elements with two antero-lateral processes - one robust abaxial process aligned rostrally and a

less robust but equally long adaxial process that extends ventrally; (iii–iv) two morphologically similar bipennate elements with short anterior processes aligned rostrally with the adaxial antero-lateral processes of the S_1 and S_2 elements, and long posterior processes aligned dorso-caudally with the outer cusps of the S_1 and S_2 elements. The ramiform array is flanked abaxially by a pair of symmetrically arranged makellate M elements that are oriented with their long, curved, inner-lateral process at about 60 degrees to the bilateral axis, converging rostrally such that their cusps are directed horizontally and laterally, and their short outer-lateral process is oriented ventrally.

Apparatus architecture

The elements within the apparatus of *Nicoraella* are arranged such that the S_0 occupies the most rostral position, on the plane of bilateral symmetry, with its paired lateral processes and cusp positioned slightly rostrad, and the rostral processes of the cusps of the S_{1-4} elements positioned slight caudad of one another. Otherwise, the S elements are all generally aligned in parallel with one another and the plane of bilateral symmetry, and at approximately 55 degrees relative to a horizontal plane. The M elements are oriented with their long axis at approximately 25 degrees relative to the S elements and approximately 45 degrees to a horizontal plane, with the tips of their cusps in line with the rostral limit of the S_0. The long axes of the P elements are aligned approximately perpendicular to the horizontal plane; following Purnell *et al.* (2000), this 'anterior-posterior' axis of the P elements equates to the ventral-dorsal (respectively) axis of the organism. The P elements are positioned at mid-height (with respect to the S elements) on this dorso-ventral axis, occluded, and with their sinistral elements positioned caudal to their dextral pair. The P_2 elements are positioned approximately halfway along the rostro-caudal axis – between the P_1 elements and the caudal 'posterior' tips of the S_{3-4} elements. The P_1 elements are positioned caudad of the P_2 and S_{0-4} elements.

Collapse simulations

We were able to validate our architectural model by observing that, when viewed from different orientations, we could simulate the collapse orientations of the component clusters. The first cluster (pm028-18-wy1-C1) contains 15 elements that are highly compressed (Fig. 2A–C), and it can be replicated by viewing the model from an oblique rostro-lateral (dextral) orientation, slightly oblique to the horizontal plane (Fig. 2D). This orientation effectively simulates the overlap between the P_1, P_2, and ramiform array, the 'parallel' arrangement of these elements, and the orthogonal relative arrangement of the P elements versus the 'anterior' (caudal) process of the M elements. Detailed differences between the model and this fused cluster, including the apparently shallower inclination

of the S_{3-4} versus the P elements, and the greater apparent separation between the S_2 versus S_{3-4} elements, can be rationalized by rotation and the apparent foreshortening of element spacing that results from collapse of the three-dimensional arrangement of the elements in the model to the two-dimensional plane represented by the cluster.

The second cluster (pm028-25-wy1-C1) is composed of 13 elements, including all anticipated except a pair of P_1 elements; the cusps of the M elements are also missing (Fig. 3A–C). This 'oblique' arrangement can be simulated by viewing the model from only a very slightly oblique lateral (dextral) perspective (Fig. 3D), including only a very minor rostral component. In this orientation, we can accurately simulate the very slight rostrad position of the dextral S and M elements with respect to their sinistral counterparts. Because the collapse orientation is almost purely lateral, the P elements do not collapse to a position in which they overlap and, therefore, fuse together with the S and M elements, and hence the P_2 elements are retained in the cluster by a large mass of diagenetic mineral, rather than through overlap with the S and M elements, and the P_1 elements are not retained at all. The model accurately reproduces the caudal separation of the S_2 from the S_{3-4} elements; this was not achieved in the first cluster and the differences in the efficacy of the model simulation reflect the degree to which the collapse orientation departs from pure lateral. We observe no significant differences between the arrangement of the elements in the model and the cluster except for the orientation of the P_2 elements which are parallel to the plane of collapse in the cluster, but approximately perpendicular to this plane in the model. This difference can be rationalised readily in terms of gravitationally induced rotation during collapse.

The third cluster (pm028-25-wy1-C2; Fig. 4A–C) preserves a parallel arrangement of the S elements, but with the cusps of the symmetrically-opposing elements displaced dextrally relative to one another. This arrangement can be simulated by viewing the model from the dextral side at about 45 degrees to the horizontal plane, with a minor caudal component; this orientation effectively simulates the arrangement of the dextral S and M elements appearing ventral of their sinistral counterparts (Fig. 4D). In detail, the M elements are directed in opposition in the cluster (Fig. 4B–C), rather than in the parallel arrangement simulated in lateral collapse orientations (Figs 2D, 3D). Our model simulation is not exact; the dextral M is oriented approximately perpendicular to the plane of collapse (Fig. 4D) and could settle gravitationally in either a parallel or opposed orientation seen in the cluster (Fig 4B–C). Similarly, the S_1 elements in our model occupy a more caudad position relative to their arrangement in this cluster. The remaining differences are accounted for by collapse, from the three-dimensional arrangement of the model to the essentially two-dimensional cluster. In this

orientation, the P elements in the model are isolated from the S-M array, precluding their overlap and fusion with the S and M elements during diagenesis; thus, the P_1 and P_2 elements are not retained within the cluster of S and M elements.

Finally, the fourth cluster (pm028-26-wy1-C1; Fig. 5A–C) includes only S and M elements and the sinistral S_4 is missing; the S elements are approximately parallel while the sinistral M element is approximately perpendicular to the alignment of the S_{1-4} elements, and the chord of the dextral M element is parallel to the S_{1-4} elements. The elements are not adpressed and, together with the preserved symmetry in their arrangement, it appears as though this cluster has undergone limited *post mortem* collapse or compression (Fig. 5B–C). The arrangement of S elements closely approximates the second cluster (Fig. 3A–C) and, similarly, it can be simulated by viewing the model from the side, with minor dorsal and rostral components (Fig. 5D). In this orientation, the P_2 elements overlap partially with the abaxial face of the dextral S_2 element (Fig. 5D), but the P_2 elements do not occur within the cluster because the elements have not undergone the collapse that would be required for the P_2 elements and the dextral S_2 element to make contact. The model cannot simulate the arrangement of the M elements which do not retain a bilateral arrangement common to that of the S_{0-4} array of elements; the M elements appear to retain a bilateral arrangement to each other, but as a paired unit they appear to have been rotated laterally through about 90 degrees relative to the S_{0-4} elements.

DISCUSSION

Comparison to other Gondolelloidea

The only member of Gondolelloidea that has been the subject of an architectural apparatus reconstruction is *Novispathodus* (Goudemand*, et al.* 2011), based on partial clusters of the S array, and borrowing insight into the relative size and position of the remaining elements from a bedding plane assemblage of *Neogondolella* (Orchard and Rieber 1999; Rieber 1980). The morphology of the element positional homologues in *Novispathodus* and *Nicoraella* are closely comparable, suggesting close phylogenetic affinity. However, the apparatus architectures show significant differences. In particular, the S array of *Novispathodus* was reconstructed to have a more caudally positioned S_0, the rostral processes of the S elements are more widely spaced than in *Nicoraella*, and their caudal processes are more tightly clustered about the plane of bilateral symmetry. The M elements are inferred to have occupied a much more dorsal and rostral position in *Novispathodus*, with their cusps converging in line with those of the S_{1-2} elements. The P_1 and P_2 elements have been located in close approximation, fully caudad of the S elements in *Novispathodus*, while in *Nicoraella* the P_2 and S

elements overlap in position on the rostral-caudal axis, and the P_1 elements occupy a distinct caudal position.

These differences might reflect taxonomic and phylogenetic differences. Certainly, since most of the clusters we describe reflect lateral collapse orientations, the alignment of the ramiform elements may not be accurately reconstructed in *Nicoraella*. Nevertheless, where critical differences occur between the inferred apparatus architectures of *Novispathodus* and *Nicoraella*, direct architectural evidence is lacking for *Novispathodus*. Indeed, many aspects of the apparatus architecture of *Novispathodus* were borrowed from *Neogondolella*, or inferred based on *ad hoc* optimality criteria, like the relative shape of the component elements within the apparatus and what this may imply about their relative positions and functions, as part of a more general 'biomechanical analysis' (Goudemand*, et al.* 2011). Unfortunately, there is no intrinsic evidence from *Novispathodus* that discriminates its apparatus architecture from our reconstruction of *Nicoraella*. Indeed, we can simulate the only architectural information for *Novispathodus* on an essentially lateral collapse of the apparatus architecture of *Nicoraella*; the natural assemblage of *Neogondolella* (Fig. 6) (Orchard and Rieber 1999; Rieber 1980; Goudemand*, et al.* 2011) can also be rationalized by viewing the *Nicoraella* model from a combined right dextro-lateral perspective (Fig. 6). Differences are evident: the M elements in *Neogondolella* occupied a more ventral position, the S_1 element a more rostral position. Nevertheless, we take the apparatus architecture of *Nicoraella* as a more accurate model for *Novispathodus* and *Neogondolella* and, therefore, for Gondolelloidea more generally.

Comparison to other conodonts

Architectural models exist principally for *Idiognathodus* (Aldridge*, et al.* 1987; Purnell and Donoghue 1997, 1998), *Promissum* (Aldridge*, et al.* 1995), *Notiodella* (Aldridge*, et al.* 2013) and *Panderodus* (Sansom *et al.* 1994). The apparatus architecture of *Nicoraella* exhibits greatest similarity to *Idiognathodus*, which has been shown also to explain natural assemblages of other polygnathaceans (Purnell and Donoghue 1998) *sensu* Donoghue *et al.* (2008), which are members of Ozarkodinina along with the Gondolelloideans (Donoghue*, et al.* 2008). In comparison to *Idiognathodus*, the apparatus architecture of *Nicoraella* is more compact, with the P_2 elements juxtaposed to the S array and the P_1 elements occupying a similar relative position to the P_2 elements in *Idiognathodus*. In this sense, the apparatus architecture of *Nicoraella* is more akin to that of *Ozarkodina remscheidensis remscheidensis* (Nicoll and Rexroad 1987) which, like *Nicoraella*, has distinctly digyrate $S_{1\text{-}2}$ elements, rather than the pseudo-bipennate but strictly extensiform digyrate $S_{1\text{-}2}$ elements of *Idiognathodus* (Purnell and Donoghue 1997).

Implications of apparatus architecture for functional hypotheses

While the history of research into conodont element functional morphology was intimately linked to debate over the biological affinity of conodonts, this changed with the discovery of soft tissue remains. Subsequent functional research was constrained by knowledge of apparatus architecture (Aldridge*, et al.* 1987; Purnell and Donoghue 1997).

More recently, Goudemand and colleagues (2011) developed a new and more detailed functional interpretation based on *Novispathodus*, founding their inferred arrangement of elements in large part on their biomechanical analysis, apparently deriving independent evidence for the existence of a lingual cartilage, as in the feeding apparatuses of the living cyclostomes. In this model they identify 'growth' and 'cluster' (functional) positions for the elements, based principally upon the complementary morphology exhibited by the elements. A lingual cartilage is imagined to have occupied a space in the arrangement of the elements that could explain movements of the elements inferred from their morphology.

However, as we have shown, the apparatus architecture of *Novispathodus* exhibits incompatibilities with that inferred for the close relative *Nicoraella*, and the primary architectural evidence for *Novispathodus* and *Neogondolella* is better explained by the apparatus architecture inferred for *Nicoraella* (e.g. the collapse orientation for Cluster 1 in Fig. 2). There is no evidence for the 'growth' arrangement of elements for the hypothetical *Novispathodus* apparatus (Goudemand*, et al.* 2011), and the apparatus architecture of *Nicoraella* is incompatible with many of the element motions proposed for *Novispathodus*. For example, the proposed location of a lingual cartilage is precluded by the arrangement of the S elements and, furthermore, much of the rotational motion inferred for the S_0 element is precluded by the ventrally and adaxially directed lateral processes of the S_2 element, as well as by the P_2 elements which are located close to the S array in the apparatus of *Nicoraella*. The proposed motion of the S_3 and S_4 elements, independently of the S_2 and S_1 elements, appears unlikely since, in our apparatus model, the S_2 elements are aligned with the S_3 and S_4 elements and, as Goudemand *et al.* (2011) argued, the S_1 elements are aligned and encapsulated by the S_2 elements.

Of course, it would be possible to develop and refine the biomechanical model of *Novispathodus* (Goudemand *et al.* 2011), accommodating the physical space constraints imposed by the architecture of the apparatus. However, this exercise has perhaps demonstrated that attempts to

infer the kinematics of the conodont feeding apparatus based primarily on the complementary morphology of the elements, and based on optimization-based functional interpretation, is not an effective approach (Purnell and Donoghue 1999).

While the functional morphology of Ozarkodinina P elements is comparatively well understood (Donoghue and Purnell 1999; Martínez-Pérez *et al.* 2014a, b, 2016), the functional interpretation of S and M elements remains the subject of speculation. These ramiforms have been conjectured to perform a role in grasping, but no material evidence has been presented in support of this interpretation, beyond analysis of element growth (Purnell 1994) and analogy based on morphological similarity (Goudemand*, et al.* 2011). Rather than guiding anatomical reconstructions, functional interpretations should be constrained by independently derived anatomical reconstructions, such as that presented here for *Nicoraella*, and they could be tested by analysis of recurrent patterns of damage and repair (Purnell and Jones 2012), or through computational and functional experiments of the loads implied by such functional interpretations.

CONCLUSIONS

The tomographic characterization of exceptional three-dimensionally preserved conodont clusters from early Middle Triassic of Luoping (southwest China) has provided the best evidence for the apparatus architecture and the relative positions of the elements of any gondolelloid, and among the best for any conodont species. The simulation of the different collapse patterns, based on the fused clusters and reproduced through our three-dimensional digital apparatus model, demonstrate the accuracy of our reconstruction. Our study demonstrates that the clusters possessed more of the original skeletal architecture that clearly reflects the relative position of each component element in the apparatus, showing distinct differences with previous proposals. These differences bring a new perspective to understanding conodont skeletal anatomy, functional morphology, and feeding kinematics. In this context, our results allow us to test the architectural and functional models of *Novispathodus* proposed previously by Goudemand *et al*. (2011), demonstrating that their model contradicts primary anatomical evidence in the fossils from which it was derived. As such, their apparatus reconstruction and their functional model must be rejected. More importantly, our study establishes the limitations of attempts to reconstruct the anatomical architecture of the conodont apparatus based on functional principles, underlining the importance of discriminating comparative anatomy and functional interpretation in inferring functional morphology in extinct organisms.

Acknowledgements. This study was supported financially by the National Natural Science Foundation

of China (41502013, 41572091), Chinese Geological Survey projects (Grant Nos. DD20160020, 12120114068001, 1212011140051, 12120114030601 and 1212010610211), State Key Laboratory of Palaeobiology and Stratigraphy (Nanjing Institute of Geology and Palaeontology, CAS) (No. 133106), and Sylvester Bradley Award (No. PA-SB201401) from the Palaeontological Association (UK). CM-P was partially founded by a Marie Curie FP7-People IEF 2011-299681, and by the Projects CGL2014-52662-P and GV/2016/102. PCJD was funded by NERC NE/G016623/1, and MJB by NERC NE/P013724/1. We received funding from the European Union's Horizon 2020 research and innovation programme under grant agreement n. 730872, project CALIPSOplus. We acknowledge the Paul Scherrer Institut, Villigen, Switzerland for provision of synchrotron radiation beamtime at the TOMCAT beamline X02DA of the Swiss Light Source and we would like to thank Dr Anne Bonnin, Dr Federica Marone, Dr Christian Schlepütz and Dr Elena Borisova for assistance.

DATA ARCHIVING STATEMENT

Tomographic data for this study are available in the Bristol Digital Repository (Huang *et al.* 2019): http://dx.doi.org/10.5523/bris.yw0swm1vgiz92catj97qv8g1c.

References

ALDRIDGE, R. J. 1987. Conodont palaeobiology: a historical review. 11-34. *In* ALDRIDGE, R. J. (ed.) *Palaeobiology of conodonts*. Ellis Horwood, Chichester, pp. Custom 7.

____ BRIGGS, D. E. G., SMITH, M. P., CLARKSON, E. N. K. and CLARK, N. D. L. 1993. The anatomy of conodonts. *Philosophical Transactions of the Royal Society of London, Series B*, **340**, 405-421.

____ MURDOCK, D. J. E., GABBOTT, S. E. and THERON, J. N. 2013. A 17-element conodont apparatus from the Soom Shale Lagerstätte (Upper Ordovician), South Africa. *Palaeontology*, **56**, 261-276.

____ PURNELL, M. A., GABBOTT, S. E. and THERON, J. N. 1995. The apparatus architecture and function of *Promissum pulchrum* Kovács-Endrödy (Conodonta, Upper Ordovician), and the prioniodontid plan. *Philosophical Transactions of the Royal Society of London, Series B*, **347**, 275-291.

____ SMITH, M. P., NORBY, R. D. and BRIGGS, D. E. G. 1987. The architecture and function of Carboniferous polygnathacean conodont apparatuses. 63-76. *In* ALDRIDGE, R. J. (ed.) *Palaeobiology of conodonts*. Ellis Horwood, Chichester, pp. Custom 7.

BRIGGS, D. E. G. and FORTEY, R. A. 1982. The cuticle of the aglaspidid arthropods, a red-herring in the early history of the vertebrates. *Lethaia*, **15**, 25-29.

____ and WILLIAMS, S. H. 1981. The restoration of flattened fossils. *Lethaia*, **16**, 1-14.

COLLINSON, C., AVCIN, M. C., NORBY, R. D. and MERRILL, G. K. 1972. Pennsylvanian conodont assemblages from La Salle County, northern Illinois. *Illinois State Geological Survey Guidebook Series*, **10**, 1-37.

DONOGHUE, P. C. J., BENGTSON, S., DONG, X.-P., GOSTLING, N. J., HULDTGREN, T., CUNNINGHAM, J. A., YIN, C., YUE, Z., PENG, F. and STAMPANONI, M. 2006. Synchrotron X-ray tomographic microscopy of fossil embryos. *Nature*, **442**, 680-683.

____ and PURNELL, M. A. 1999. Mammal-like occlusion in conodonts. *Paleobiology*, **25**, 58-74.

____ ____ ALDRIDGE, R. J. and ZHANG, S. 2008. The interrelationships of 'complex' conodonts (Vertebrata). *Journal of Systematic Palaeontology*, **6**, 119-153.

GOUDEMAND, N., ORCHARD, M. J., URDY, S., BUCHER, H. and TAFFOREAU, P. 2011. Synchrotron-aided reconstruction of the conodont feeding apparatus and implications for the mouth of the first vertebrates. *Proceedings of the National Academy of Sciences of the United States of America*, **108**, 8720-8724.

HU, S. X., ZHANG, Q. Y., CHEN, Z. Q., ZHOU, C. Y., LU, T., XIE, T., WEN, W., HUANG, J. Y. and BENTON, M. J. 2011. The Luoping biota: exceptional preservation, and new evidence on the Triassic recovery from end-Permian mass extinction. *Proc Biol Sci*, **278**, 2274-82.

HUANG, J., HU, S., ZHANG, Q., DONOGHUE, P. C. J., BENTON, M. J., ZHOU, C., MARTÍNEZ-PÉREZ, C., WEN, W., XIE, T., CHEN, Z.-Q., LUO, M., YAO, H. and ZHANG, K. 2018a. Gondolelloid multielement conodont apparatus (*Nicoraella*) from the Middle Triassic of Yunnan Province, southwestern China. *Palaeogeography, Palaeoclimatology, Palaeoecology*.

____ MARTÍNEZ-PÉREZ, C., HU, S., ZHANG, Q., ZHANG, K., ZHOU, C., WEN, W., XIE, T., BENTON, M. J., CHEN, Z.-Q., LUO, M. and DONOGHUE, PHILIP C. J. 2019. Data from: Apparatus architecture of the conodont *Nicoraella kockeli* (Gondolelloidea, Prioniodinina) constrains functional interpretations.

____ ____ ____ DONOGHUE, P. C. J., ZHANG, Q.-Y., ZHOU, C.-Y., WEN, W., BENTON, M. J., LUO, M., YAO, H.-Z. and ZHANG, K.-X. 2018b. Middle Triassic conodont apparatus architecture revealed by synchrotron X-ray microtomography. *Palaeoworld*.

____ ZHANG, K., ZHANG, Q., LÜ, T., HU, S. and ZHOU, C. 2011. Advance research of conodont fauna from Shangshikan and Daaozi sections in Luoping area, Yunnan Province. *Geological Science and Technology Information*, **30**, 1-17.

____ ____ ____ ____ ZHOU, C. and BAI, J. 2009. Conodonts stratigraphy and sedimentary environment of the Middle Triassic at Daaozi section of Luoping County, Yunnan Province, south China. *Acta Micropalaeontologica Sinica*, **26**, 211-224.

MARONE, F., MÜNCH, B. and STAMPANONI, M. 2010. Fast reconstruction algorithm dealing with

tomography artifacts. 780410. *SPIE Proceedings ''Developments in X-Ray Tomography VII''*.

MARTÍNEZ-PÉREZ, C., PLASENCIA, P., JONES, D., KOLAR-JURKOVŠEK, T., SHA, J., BOTELLA, H. and DONOGHUE, P. C. J. 2014a. There is no general model for occlusal kinematics in conodonts. *Lethaia*, **47**, 547-555.

____ RAYFIELD, E. J., BOTELLA, H. and DONOGHUE, P. C. J. 2016. Translating taxonomy into the evolution of conodont feeding ecology. *Geology*, **44**, 247-250.

____ ____ PURNELL, M. A. and DONOGHUE, P. C. J. 2014b. Finite element, occlusal, microwear and microstructural analyses indicate that conodont microstructure is adapted to dental function. *Palaeontology*, **57**, 1059-1066.

MASTANDREA, A., IETTO, F., NERI, C. and RUSSO, F. 1997. Conodont biostratigraphy of the late Triassic sequence of Monte Cocuzzo (Catena Costiera, Calabria, Italy). *Rivista Italiana di Paleontologia e Stratigrafia*, **103**, 173-182.

NICOLL, R. S. 1982. Multielement composition of the conodont *Icriodus expansus* Branson & Mehl from the Upper Devonian of the Canning Basin, Western Australia. *BMR Journal of Australian Geology and Geophysics*, **7**, 197-213.

____ 1985. Multielement composition of the conodont species *Polygnathus xylus xylus* Stauffer, 1940 and *Ozarkodina brevis* (Bischoff and Ziegler, 1957) from the Upper Devonian of the Canning Basin, Western Australia. *Bureau of Mineral Resources Journal of Australian Geology and Geophysics*, **9**, 133-147.

____ and REXROAD, C. B. 1987. Re-examination of Silurian conodont clusters from northern Indiana. 49-61. *In* ALDRIDGE, R. J. (ed.) *Palaeobiology of conodonts*. Ellis Horwood, Chichester, pp. Custom 7.

ORCHARD, M. J. and RIEBER, H. 1999. Multielement *Neogondolella* (Conodonta, upper Permian - middle Triassic). *Bollettino della Società Paleontologica Italiana*, **37**, 475-488.

PURNELL, M. A. 1994. Skeletal ontogeny and feeding mechanisms in conodonts. *Lethaia*, **27**, 129-138.

____ and DONOGHUE, P. C. J. 1997. Skeletal architecture and functional morphology of ozarkodinid conodonts. *Philosophical Transactions of the Royal Society of London, Series B*, **352**, 1545-1564.

____ ____ 1998. Skeletal architecture, homologies and taphonomy of ozarkodinid conodonts. *Palaeontology*, **41**, 57-102.

____ ____ 1999. Flattened fossils, physical modelling and the restoration of collapsed skeleton. 91-99. *In* SAVAZZI, E. (ed.) *Functional morphology of the invertebrate skeleton*. John Wiley & Sons Ltd., Chichester, pp. Custom 7.

____ ____ ALDRIDGE, R. J. 2000. Orientation and anatomical notation in conodonts. *Journal of*

Paleontology, **74**, 113-122.

____ and JONES, D. O. 2012. Quantitative analysis of conodont tooth wear and damage as a test of ecological and functional hypotheses. *Paleobiology*, **38**, 605-626.

RIEBER, H. 1980. Ein conodonten-cluster aus der Grenzbitumenzone (Mittlere Trias) des Monte San Giorgio (Kt. Tessin/Schweiz). *Ann. Naturhist. Mus. Wien*, **83**, 265-274.

SANSOM, I. J., ARMSTRONG, H. A. and SMITH, M. P. 1994. The apparatus architecture of *Panderodus* and its implications for coniform conodont classification. *Palaeontology*, **37**, 781-799.

SCHMIDT, H. 1934. Conodonten-Funde in ursprünglichem zusammenhang. *Paläontologische Zeitschrift*, **16**, 76-85.

SCHÜLKE, I. 1997. Conodont clusters and multielement reconstructions from the Upper Kellwasser horizon at La Serre (Late Frasnian, Montagne Noire, Southern France). *Geologica et Palaeontologica*, **31**, 37-66.

SCOTT, H. W. 1934. The zoological relationships of the conodonts. *Journal of Paleontology*, **8**, 448-455.

ZHANG, Q.-Y., ZHOU, C.-Y., LU, T., XIE, T., LOU, X.-Y., LIU, W., SUN, Y.-Y., HUANG, J.-Y. and ZHAO, L.-S. 2009. A conodont-based Middle Triassic age assignment for the Luoping Biota of Yunnan, China. *Science in China Series D: Earth Sciences*, **52**, 1673-1678.

FIGURE CAPTIONS

FIG. 1. *Nicoraella kockeli* conodont apparatus architecture and notation reconstructed from the fused clusters natural assemblages described here, using virtual models of the elements from cluster pm028–18–wy1–C1 (Fig. 2A–C). A, lateral; B, rostral; C, dorsal; and D, caudal views of the apparatus

FIG 2. Isosurface and segmented model of the *Nicoraella kockeli* cluster pm028–18–wy1–C1 derived from SRXTM data containing the 15 elements of the apparatus. Scale bar represents 400 µm. A, Isosurface models of the cluster; B–C, segmented model in left and right views; D, virtual model of the reconstructed apparatus simulating the direction of collapse.

FIG 3. Isosurface and segmented model of the *Nicoraella kockeli* cluster pm028–25–wy1–C1 derived from SRXTM data containing 13 elements of the apparatus. Scale bar represents 400 µm. A, Isosurface models of the cluster; B–C, segmented model in left and right views; D, virtual model of the reconstructed apparatus simulating the direction of collapse.

FIG 4. Isosurface and segmented model of the *Nicoraella kockeli* cluster pm028–25–wy1–C2 derived from SRXTM data containing 11 elements of the apparatus. Scale bar represents 400 µm. A, Isosurface models of the cluster; B–C, segmented model in anterior oblique and left and lateral (slightly dorsal) views respectively; D, virtual model of the reconstructed apparatus simulating the direction of collapse.

FIG 5. Isosurface and segmented model of the *Nicoraella kockeli* cluster pm028–26–wy1–C1 derived from SRXTM data containing 11 elements of the apparatus. Scale bar represents 400 µm. A, Isosurface models of the cluster; B, segmented model in lateral (slightly ventral) view; C, segmented model in almost lateral view; D, virtual model of the reconstructed apparatus simulating the direction of collapse.

FIG 6. Comparison between A, the *Neogondolella* natural assemblage from the Middle Triassic at Monte San Giorgio, Switzerland (camera lucida sketch of the natural assemblage of *Neogondolella* based on text–fig. 2B of Goudemand et al., 2011). Scale bar represents 400 µm, and B, the simulation of the collapse pattern based on our reconstruction of the apparatus of *Nicoraella kockeli*.

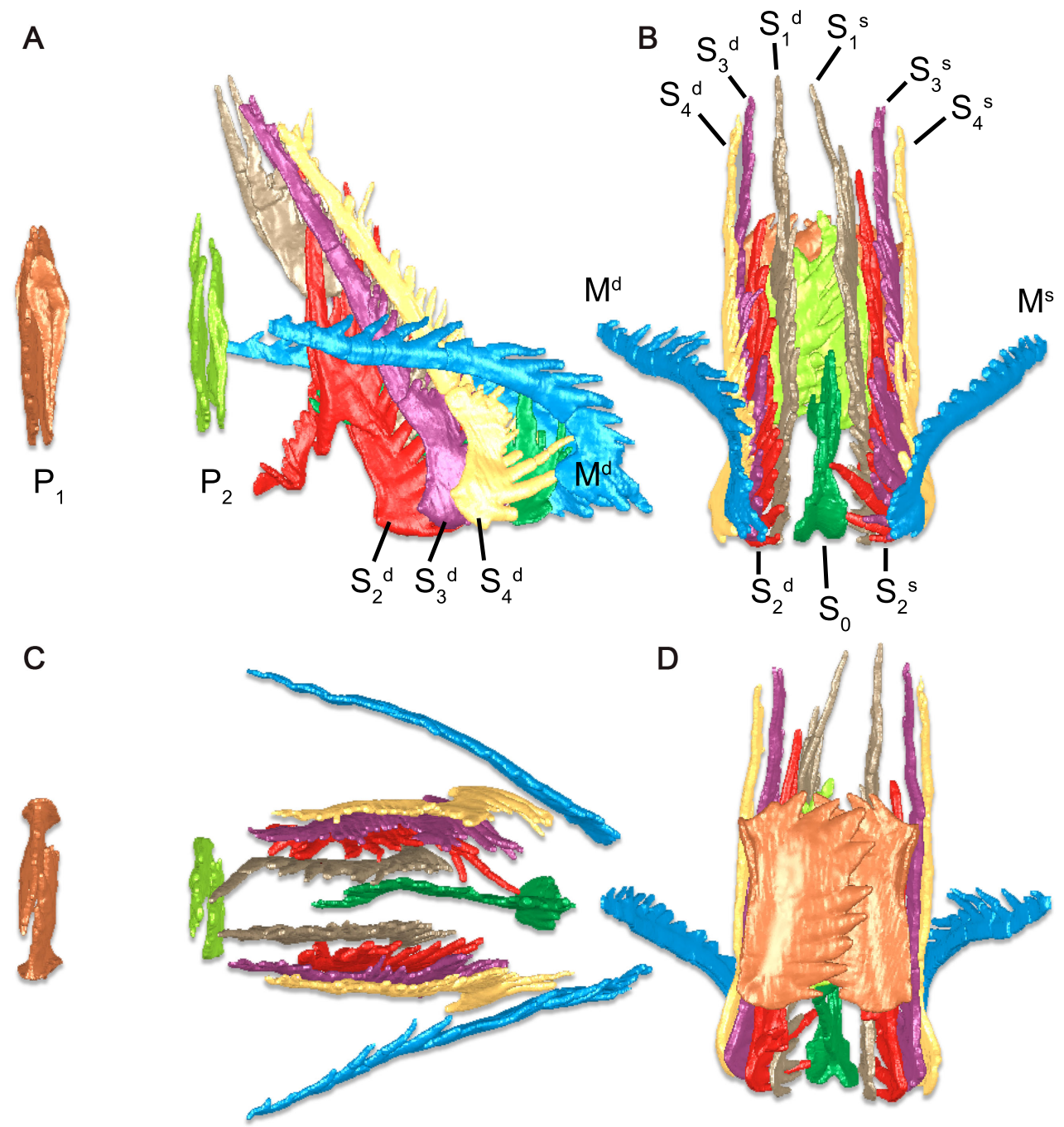
A
B
C
D
P1
P2
Md
Ms
S1d
S1s
S2d
S2s
S3d
S3s
S4d
S4s
S0

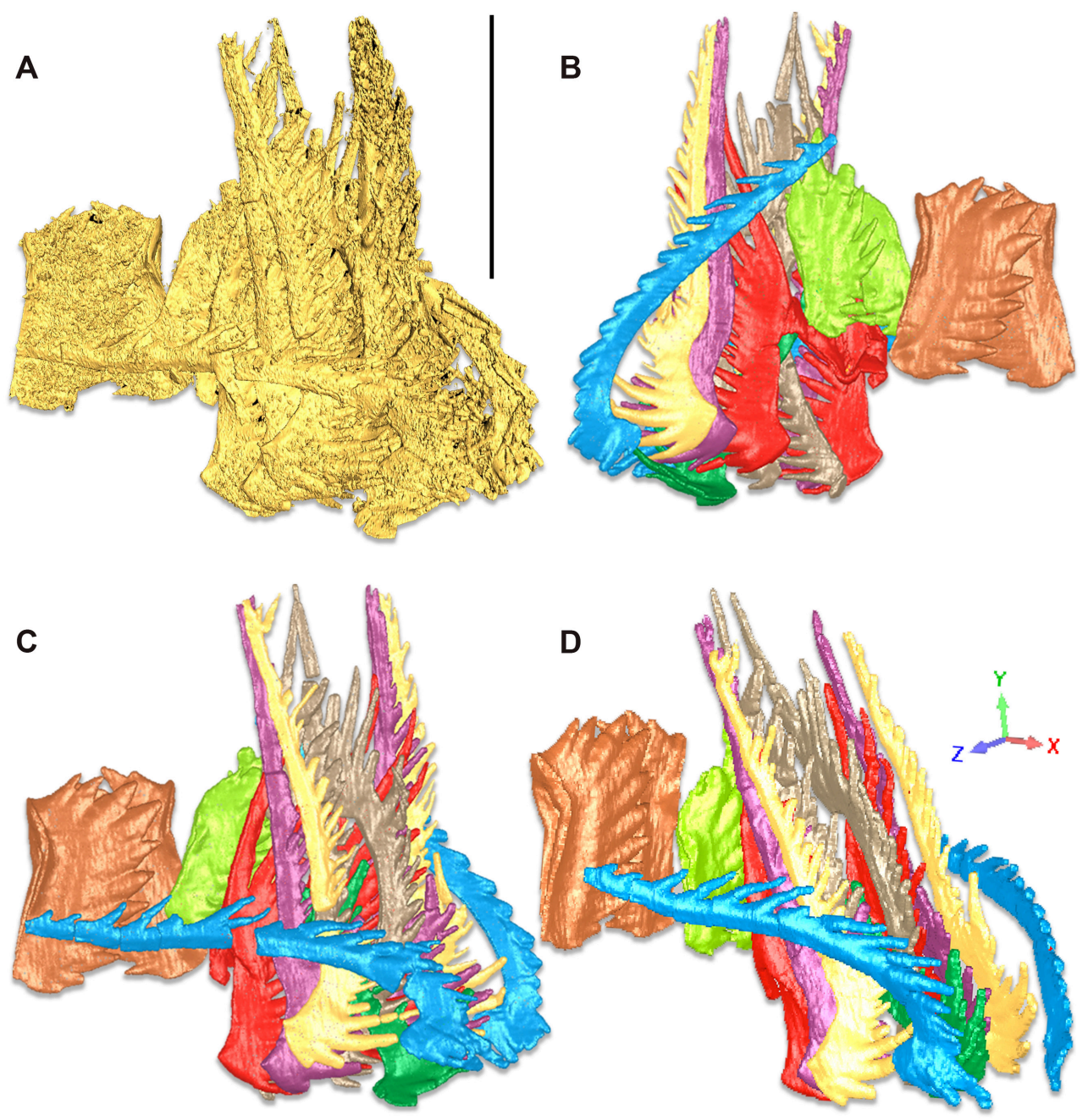
A
B
C
D
Y
Z
X

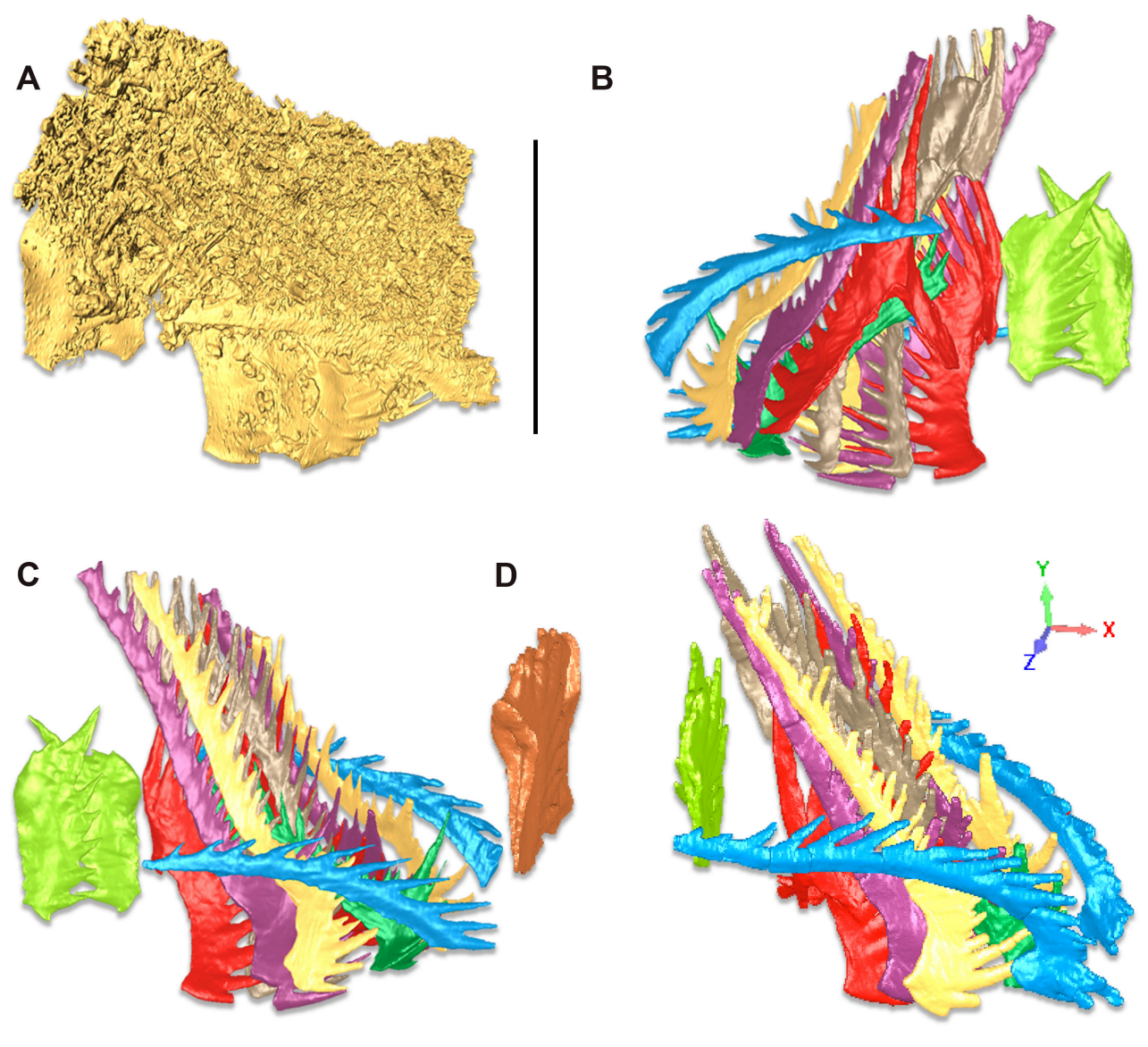
A
B
C
D
Y
X
Z

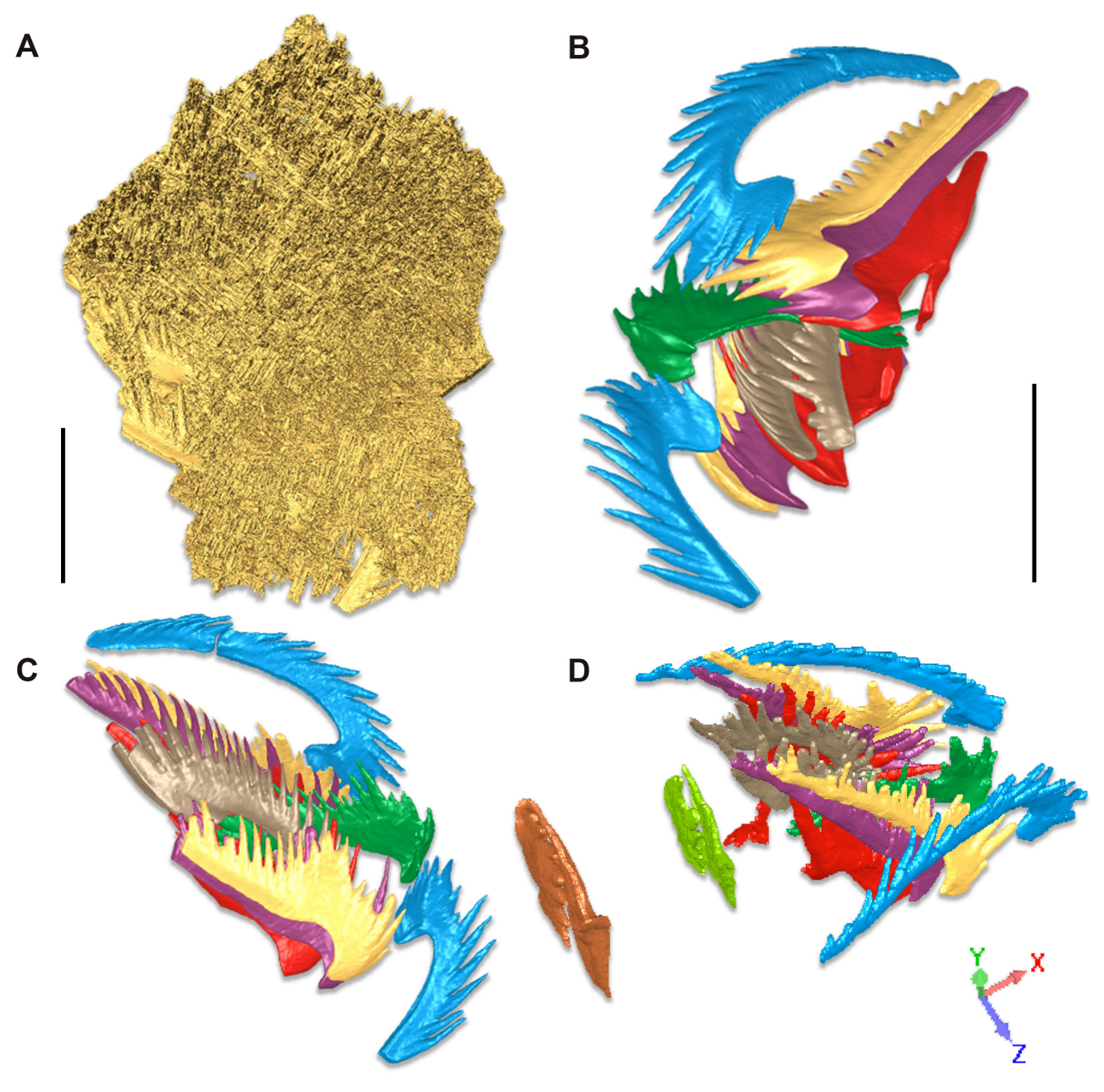
A
B
C
D
Y
X
Z

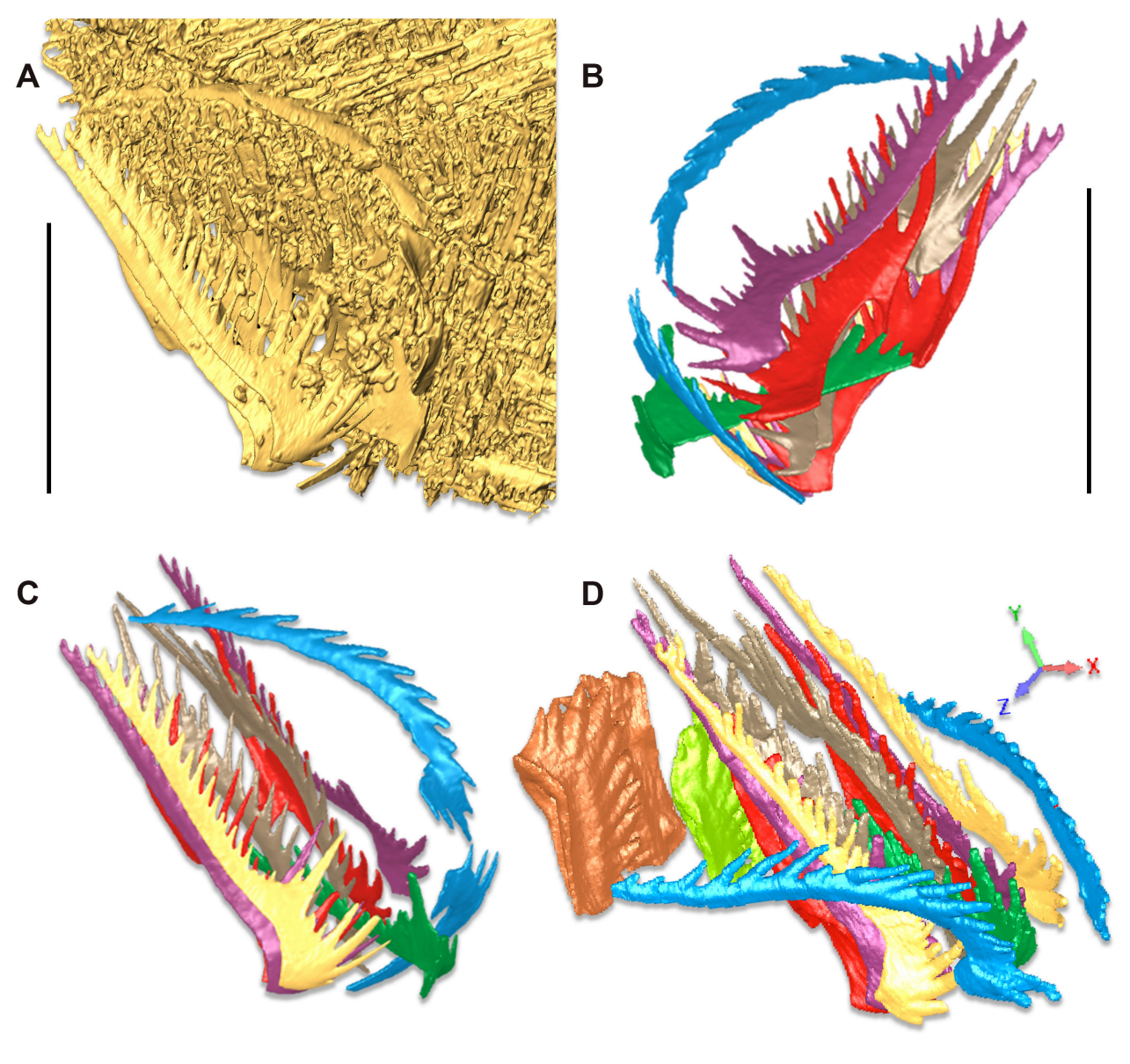
A
B
C
D
Y
X
Z

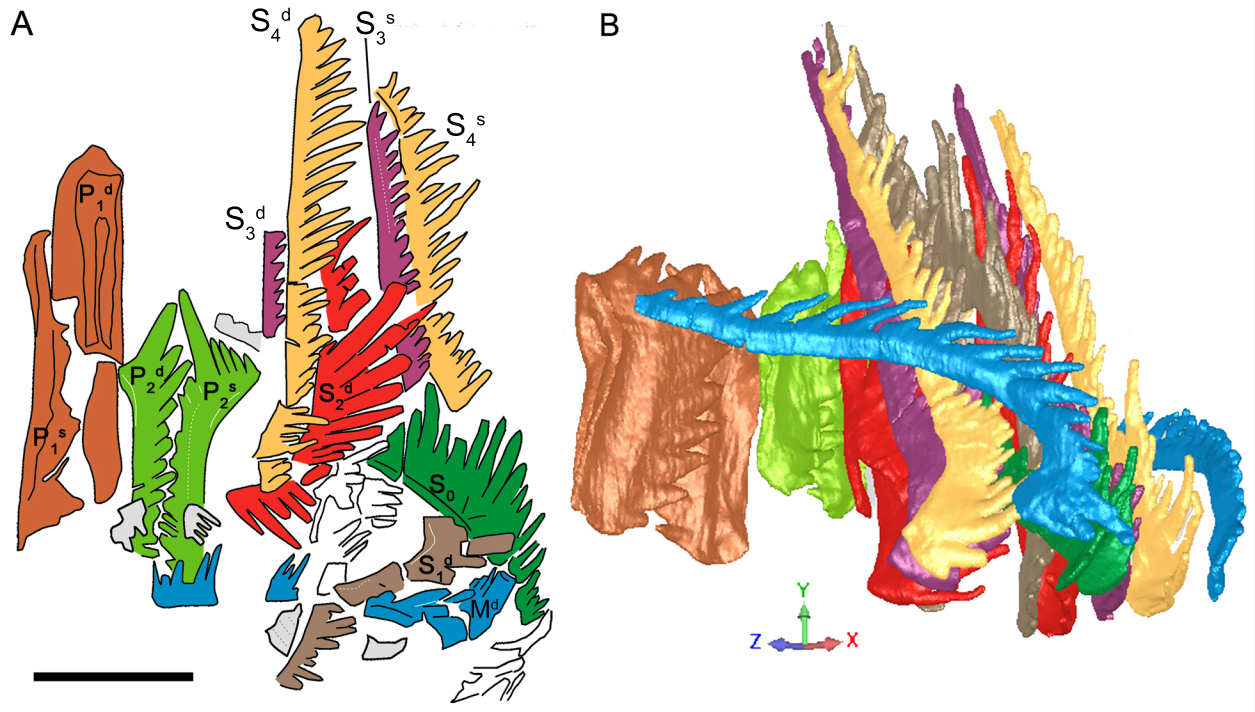
A
S_4^d
S_3^s
S_4^s
S_3^d
P_1^d
P_2^d
P_2^s
P_1^s
S_2^d
S_0
S_1^d
M^d
B
Y
Z
X